Engineering and Technology Journal
Journal homepage: https://etj.uotechnology.edu.iq

Synthesis of Porous Silicon by Electrochemical Etching for Gas Sensor Application

Duha H. Jwied [a*], Uday M. Nayef [b], Falah AH Mutlak [c]

[a'b] Applied Sciences Dept., University of Technology-Iraq, Alsina'a street, 10066 Baghdad, Iraq.
[c] College of Science, University of Baghdad, Baghdad, Iraq
*Corresponding author Email: duhahadi86@yahoo.com

HIGHLIGHTS

- Preparation of porous Silicon (PS) by Electrochemical etching method.
- Study of structural, morphological, and electrical properties for porous Silicon.
- Fabrication of Al/PS/Si/Al as gases sensor.

ARTICLE INFO

Handling editor: Rana F. Ghani

Keywords: Porous Silicon; Electrochemical etching method; X-Ray Diffraction; gas sensor.

ABSTRACT

In the present study, the layers of porous Silicon (PS) have been produced from the p-type Silicon with a (100) orientation using the approach of electrochemical etching. The samples were anodized in a solution of HF concentration 18% and 99% C_2H_2OH. Samples characteristics of PS were studied by etching time constant (15 min). In addition, the alteration of the current density value into (5, 10,15,20, and 25) mA/ cm^2 was also studied. Samples were characterized by nanocrystalline porous Silicon via X-Ray Diffraction (XRD). The AFM (Atomic force microscope) analysis of PS shows the sponge-like structure. Also, a 39.76 nm average diameter was coordinated in the rod-like temperature variation, fabricated from prepared samples on the sensor's sensitivity, recovery time, and response time. The maximal level of the sensitivity has been approximately (20,11)% for porous Silicon of gas NO_2 and NH_3, respectively.

1. Introduction

The PS composites provide modified functionality compared to the as-prepared PS and expand the applicability. The formations of the layers of the PS on the crystalline Silicon wafers utilize the electrochemical etching ECE. This highly simple and reliable method has been utilized for synthesizing the PS [1]. PS can be defined as one of the significant materials in the sensor technologies due to its various applications in analyses detection [2]. The 'anodization' and the 'anodic etching' terms were utilized to describe the formation of the pores. This is because the semiconductor plays the role of an anode in the electrochemical reaction, where the atoms of the Silicon are separated from the crystal. Various approaches have been developed for the manufacturing of the porous Silicon, including spark erosion, electrochemical anodization [3], and stain etching, vapor etching, and sol-gel approaches. Particularly, electrochemical anodization etching has been considered the most common approach for manufacturing porous Silicon. Generally, the illustrative equation of the general process throughout the PS ECE process may be represented as [3]:

$$Si + 2HF + 2h+ \rightarrow SiF2 + 2H+ \quad (1)$$

$$SiF2 + 4HF \rightarrow H2 + H2SiF6 \quad (2)$$

Based on the chemical reaction equation, there are 2 main parameters affecting the fabricated porous silicon film's etching rate: the hole (h+) concentration of the utilized Silicon-wafer and the other is HF-based solution's electrolyte concentration [4]. Porous silicon nanoparticles have been widely developed for different biomedical uses, for example, cancer cell imaging, biosensors, drug delivery, radiotherapy, and photo thermal therapy because of their easy surface modification and optical properties [5]. Electrochemical is an easy method for porous silicon formation which employs a gold cathode and silicon wafer anode immersed in hydrofluoric acid (HF) electrolyte with a constant current source, which is usually implemented to ensure steady tip concentration of HF resulting in a more homogenous porosity layer [6]. Porosity has emerged as an effective feature

http://doi.org/10.30684/etj.v40i4.2064
Received 16 March 2021; Accepted 29 May 2021; Available online 25 April 2022
2412-0758/University of Technology-Iraq, Baghdad, Iraq

that controls the electronic and optical properties of Si quantum structures. The characteristics of the surface strongly affect the properties of Si. Therefore, the quantum confinement effects are considered to control the mechanism of the luminescence in nanocrystalline [7]. The porous silicon application as a sensor involves various sensor types like the optical sensor. The optical sensing-based PS layer is a variation in the optical characteristics due to the interactions between the layer of the porous Silicon, and solvent solution vapors that may be considered as PS is an inexpensive and convenient optical device for detecting the organic solvents [8-9]. The porous Silicon has a distinctive characteristic, which makes it attractive for those applications, including an increase in the surface interaction area, simplicity, and repeatability of the compatibility and fabrication with the well-established [10]. Porous silicon (PS) is characterized as a semiconductor matrix co. The morphology, structure, and chemical composition of PSi depend strongly on chemical reactions between HF and silicon. These reactions are affected by the type of conductivity, wafer resistivity, current density, type of dopant, and solution composition. [11].

2. Experimental details

2.1 Porous silicon preparation

Porous silicon samples were prepared from a single-crystalline orientation of a p-type silicon wafer (100) and with a resistivity of 1.50-4Ω.cm (Germany made) [12]. All chemicals, hydrofluoric acid, and ethanol alcohol were purchased from Sigma Aldrich (Malaysia).

Before the Electrochemical etching process, the silicon wafers were rinsed with ethanol and action to remove dirt for removing the native oxide layer and dried by air. Then, the sample was etched in an electrolyte containing Ethanol (C_2H_5OH 99.9%). The concentration of the HF acid in this solution was 18%, a current density (5, 10, 15, 20, and 25mA/cm²) for a 15min etching time. The ethanol has been utilized in the electrolyte to reduce the surface tension and improve the homogeneity porous silicon layer by promoting the removal of the hydrogen bubble. Teflon cell resistant to the hydrofluoric acid was used to achieve the anodization etching as shown in Fig (1) The sample of the Silicon plays the role of the anode. In contrast, the cathode has a gold mesh that has resistance to the hydrofluoric acid. The conducting material after the anodization sample was rinsed in ethanol and pentane and dried with the use of nitrogen.

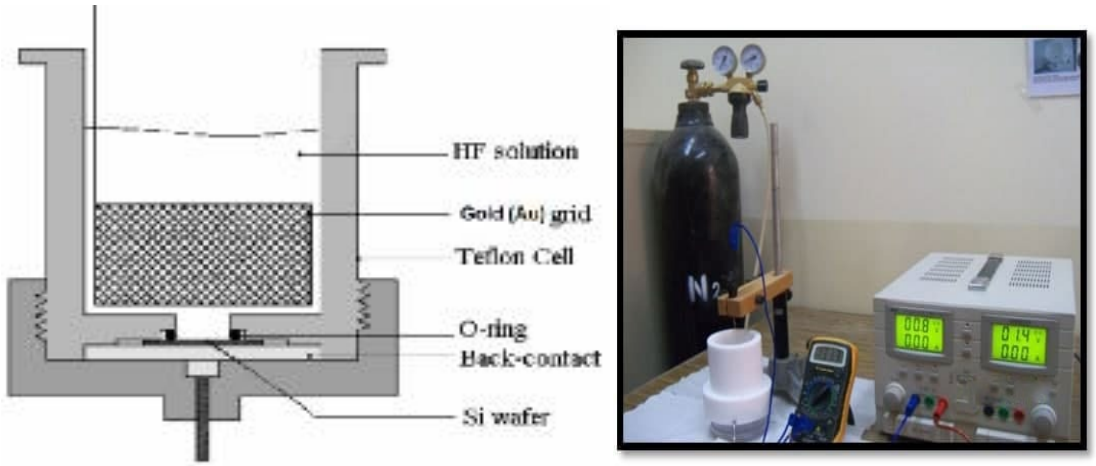

Figure 1: Schematic diagram of the porous silicon anodization

2.2 Gas sensor

Thermal evaporation deposited aluminum electrodes on a surface for samples. Prepared samples were tested as gas sensors. The gas sensing mechanism depends on surface reaction for chemisorbed oxygen, oxidation, and gas reduction. There are two forms of oxygen adsorption on a film surface: physisorption and chemisorption. Chemisorption is dominant at higher temperatures. The transition from physisorption to chemisorption requires activating energy that increases operating temperature can accomplish. The amount of oxygen adsorbed on a sensor surface increased as the temperature increased. Electric physicals and gas sensing properties of PS films between (100-300) temperature range are dominated via molecular oxygen and atomic oxygen, where oxygen is adsorbed on metal oxide surface, allowing electron trapping. Therefore, the density for load carriers is reduced, increasing PS resistance. The following reaction is possible:

$$O_2\,(atm) + 2e^-\,(cond\ band) \rightarrow 2O^-(ads) \qquad (3)$$

O^- is the chemisorbed oxygen, and e- is the pinned electrons for the surface of PS, where O_2 is an adsorbed oxygen molecule. O^- Surface species act as electron receivers and cause a depletion layer that extends both to particles and a surface Barrie. Gas sensitivity can be calculated from the following relationship:

$$\text{S}\,\% = (\text{Ron}\,(\Omega)\text{-Roff}\,(\Omega))/\text{Ron}\,(\Omega) \times 100\% \qquad (4)$$

Response time and recover time was also measured as follows:

$$\text{Response time (sec)} = \text{ABS ((t gas (on) - t gas (off)) } \times 0.9) \quad (5)$$

$$\text{Recover time (sec)} = \text{ABS ((t gas (off) - t gas recover) } \times 0.9) \quad (6)$$

3. Results and discussion

3.1 XRD analyses

Patterns of XRD silicon and PS are shown in Figure (2). A separate distinction between the bulk and porous Silicon is that the peak is broad. This is because the mismatch between the Silicon and the porous Silicon is wide, so in the porous Silicon, the ray diffraction between pores is caused by nano-sized crystals. Thus, it can be confirmed that the porous silicon layer stays crystalline. However, it is somewhat pushed towards a smaller angle of diffraction. PS .

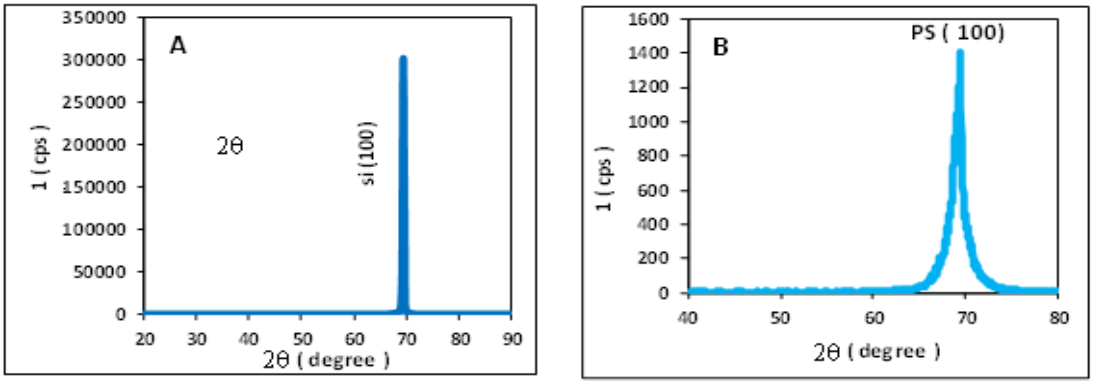

Figure 2: XRD pattern of (A) c-Si, (B) PS layer preparing at 15 mA/cm^2, etching time 15 min and HF$_C$ 18%

This result is the effect of a strain that results in a little expanded lattice parameter. After that, it pushes the porous Silicon's peak to a small diffraction angle and decreases the crystalline size. As reported by Nayef et al. [13]. The crystallite size of PS was calculated through the DebySherrer formula, and the size was equal to (16.1nm).

$$D=\frac{0.9\lambda}{\beta cos\theta} \quad (7)$$

Where D is the Nanocrystal diameter, λ is the wavelength of light, β is the peak in radian of the full width half maximum (FWHM), and ϴis the angle of Bragg.

3.2 AFM

AFM has been utilized to examine the surface morphology of porous silicon samples. AFM measurement was focused on the morphological at a nonmetric scale of the PS layers. The AFM images of the structure of the porous Silicon that obtained for a variety of the current densities (5, 15, and 25 mA/cm^2) at a scan area of 500nm x 500nm of PS layer p-type, with constant etching time at 15 min and 18% HF concentration, as shown in Figure (3). The Surface and distribution of the diameter values of the prepared samples of the PS under various current densities of the PS in which randomly distributed and irregular nanocrystalline Si pillars and voids over the whole surface may be observed. This Figure exhibits that PS with tightly branched pores has a sponge-like structure with diameters ranging from 24.98 - 39.76 nm. Morphology properties of the PS samples are shown in Table (1) when an average pore diameter shows in good agreement with the classification of the mesoporous. Table (1) also indicates that the increase in density increases the average diameter of the pores. As the current (5, 15, 25 mA/cm^2) increases, the average pore diameter increases due to increased Si dissolution occurring in the porous layer.

Table 1: Results of AFM images for PS

Samples	Average Diameter(nm)	Average Roughness (nm)
PS (5mA/cm^2)	24.98	1.48
PS (15mA/cm^2)	33.46	1.92
PS (25mA/cm^2)	39.76	2.79

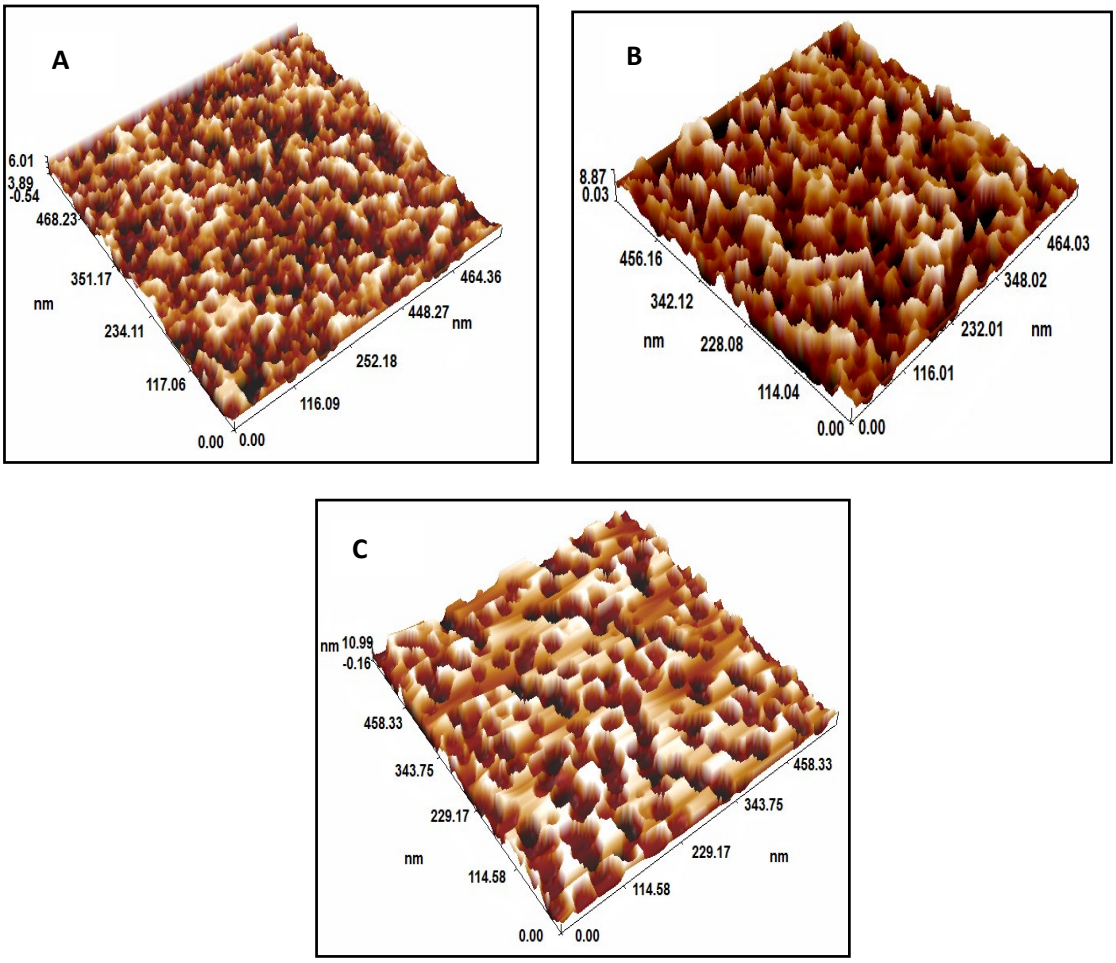

Figure 3: AFM images of PS at etching current density (A) 5, (B) 15 and (C) 25 mA/cm^2, etched time 15 min and HFc= 18%

3.3 J-V properties

Figure (4) studies *J-V* properties in Dark of c-Si and PS at different current densities for the etching and applies biases and reverse voltage at range−5 to +5V. Curves of the measuring output current were obtained. In comparison to PS, c-Si has a higher output current than PS. In the PS samples, we can see the output current diminution as a current density increases for the etching due to increased resistivities (c-Si and PS) and thickness for the PS layer. Ideality factor and barrier height Φ_{Bn} of PS/c- Si sandwich structureand their values are tabulated in Table 2 can study by *J-V* measurement according to the following equation [14]:

$$n = (q/K_BT)\,(dv/d\,(1n\,J)) \qquad (8)$$

$$\Phi_{Bn} = (K_BT/q)\ Ln\ (A^{**}T^2/J) \qquad (9)$$

Where V: represents the applied voltage, J represents forward current density (μA/cm^2), kB: represents the Boltzman constant (1.38x10^{-23} J/K), A** (32 for p-type Silicon) represents Richardson constant (A/cm^{2}K) [15-16].

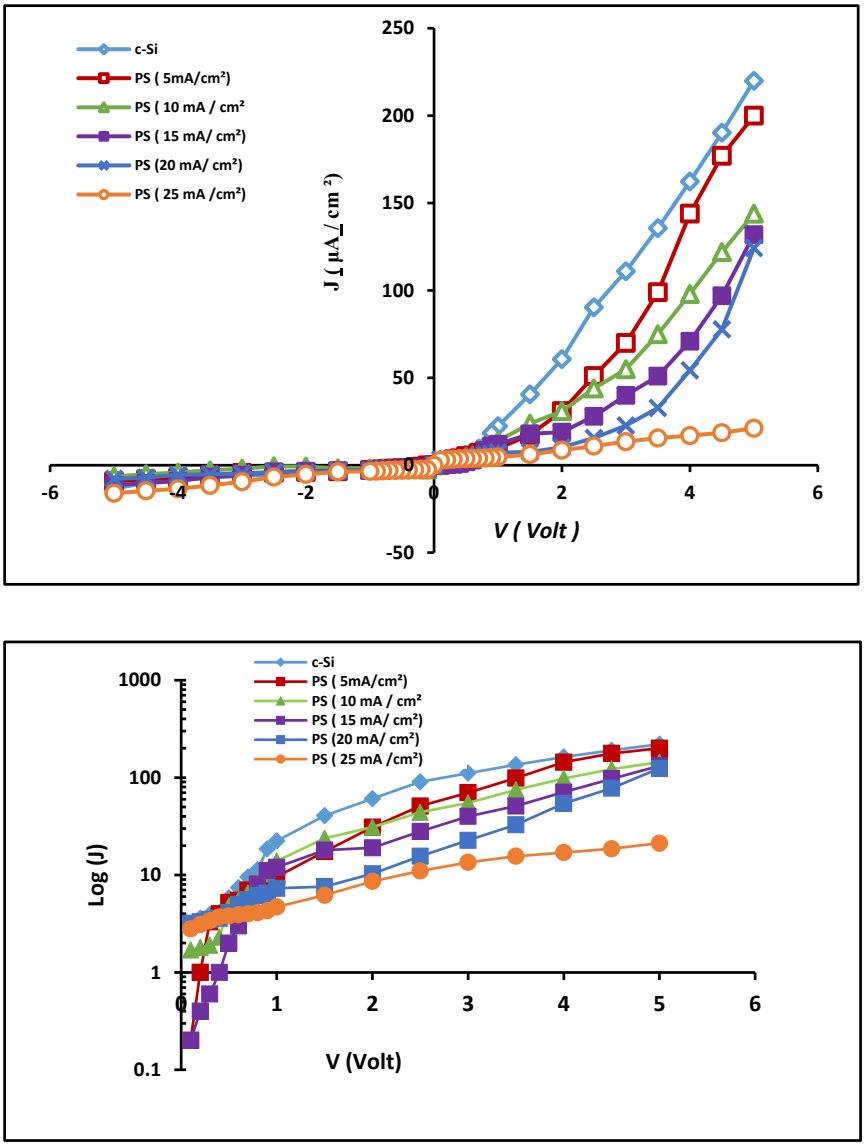

Figure 4: *J-V* characteristics of c-Si and PS prepared with different current densities 5, 10, 15, 20, and 25mA/cm^2 etching time 15min and HF_c 18%

Table 2: The study results from c-Si and PS, ideality Factor value (n), barrier-height (Js) derived from *J-V* characteristics Fig (4) with various current densities (j), at the etching time15min and 18 %

Sample			J_s (µA/cm^2)	n	Φ_{Bn} (eV)
c-Si			80	1.54	0.628
PS	J mA/cm^2	5	50	3.09	0.641
		10	20	4.96	0.604
		15	55	1.65	0.638
		20	40	2.89	0.646
		25	45	2.06	0.643

Figure (5) represents the *J-V* characteristics illumination with various power intensity values (5, 20, 60, and 125mW/cm^2) at room temperature of the Al/PS/p-Si/Al sandwich structure. The photocurrent curves have been obtained by applying a varying reverse bias (between 0V and -3V) and measuring the output current. When the structures are illuminated, the electron-hole pairs are formed in depletion of PS/c-Si. In forward bias, this will not have any effect because the current is limited by the resistance of the PS layer. However, in the reverse bias, the current increases, especially at a high voltage where the barrier is the main illumination for the current. In addition, it is noticed that increasing the light intensity results increase the photocurrent. This can be ascribed to increasing the generated photo carriers. Consequently, an increasing PS porosity and thickness of the sample and decreasing conductivity the same can be seen with the current density.

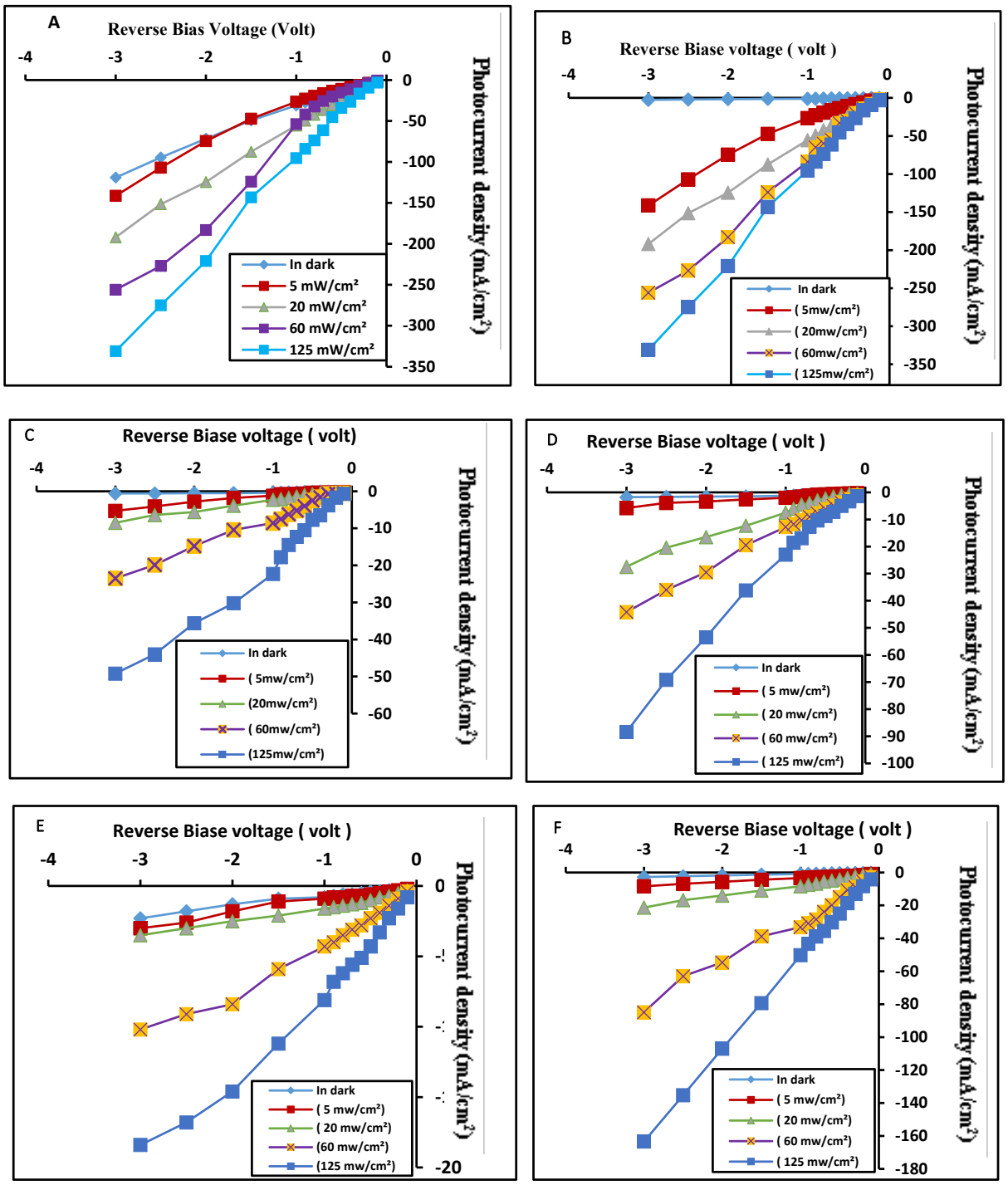

Figure 5: J_{ph}-V proprties under illumination for (a) c-Si and PS samples with different current densities (b) J=5, (c) J=10, (d) J=15, (e) J=20, and (f) J=25 mA/cm^2 at etching time 15min and HF_c=18%

3.4 Gas sensor

Figures (6) show the sensitivity as an operating temperature function in the range between (100ºC and 300ºC) for the porous silicon (15min) substrate. The results show that the sensitivity decreased with increasing operating temperature up to 200ºC and slowly increased. The porous Silicon has a higher level of sensitivity in the operating temperature of up to 100ºC-150ºC for NO_2 gas (20.3%) and (11.26%) for NH_3 gas. It can be seen from the figure that the surface area of the thin films has been increased when Porous Silicon is made, which has increased the surface area increased NO_2 and NH_3 gases sensitivities. The higher sensitivity may be attributed to the optimum number of misfits on the surface, porosity, largest surface area, and the larger rate of NO_2 oxidation and reduction of NH_3. Figure (7) show the Response time is a sample response time of gas. Also, time recovery is the time a sample consumes to return to the normal state, i.e., a sample state before pump gas. Response time variation and time alteration recovery for ps are shown in Tables 3 and 4.

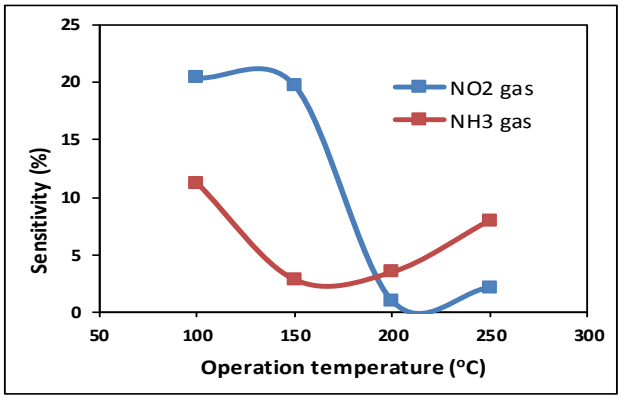

Figure 6: Sensitivity for PS prepared at current density 15mA/cm^2, etching time 15min. and HFc 18%

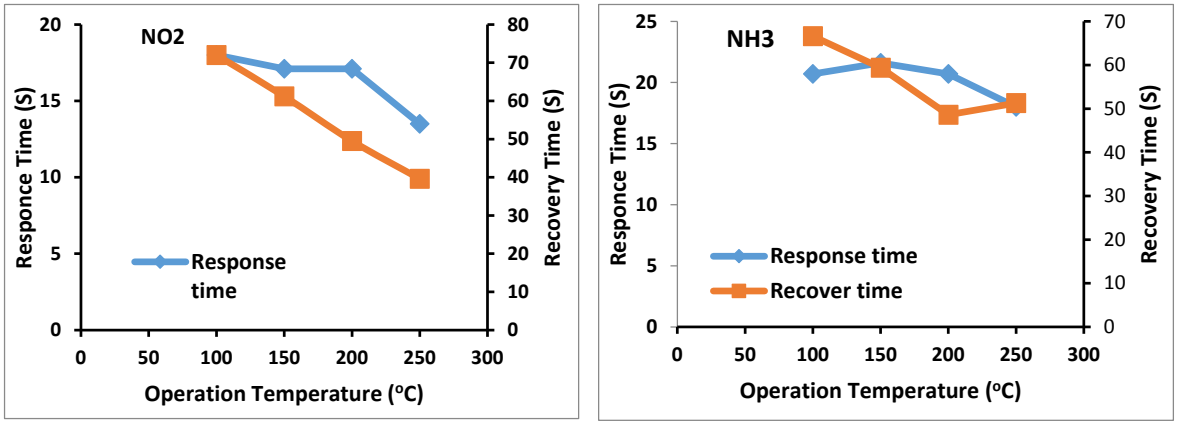

Figure 7: Response and recovery time of PS samples prepared at current density 15mA/cm^2, etching time 15min. and HF_c 18%

Table 3: Values of R (Ω) before and after exposure to NO_2 gas, sensitivity(S %), response time, and recover time (sec) for PS sample

Samples	T (°C)	(Rg) (Ω)	(Ra)(Ω)	S (%)	Response time (sec)	Recover time (sec)
J 15(mA/cm^2)	100	0.247	0.222	11.26126126	20.7	66.6
	150	230.1	223.7	2.860974519	21.6	59.4
	200	165.2	159.6	3.50877193	20.7	48.6
	250	93	86.1	8.013937282	18	51.3

Table 4: Values of R (Ω) before and after exposure to NH_3 gas, sensitivity (S %), response time, and recover time (sec) for PS sample

Samples	T (°C)	(Rg) (Ω)	(Ra)(Ω)	S (%)	Response time (sec)	Recover time (sec)
J 15(mA/cm^2)	100	0.216	0.26	20.37037037	18	72
	150	201.8	241.6	19.72249752	17.1	61.2
	200	180.2	178.4	0.998890122	17.1	49.5
	250	105.2	107.5	2.186311787	13.5	39.6

4. Conclusions

When preparing porous Silicon (PS) via Electrochemical etching (ECE), various current densities results conclude with current density in the ECE method can be considered extremely useful tools to prepare PS for gas sensor application. The structure of the PS has been formed by the anodization hydrofluoric etching of the p-type (100) Si wafers. The study of the electrical characteristics has revealed that the porous layer's resistivity is considerably larger than that of the crystalline Si. Such resistivity increases with the increase of current density. The maximum variation of resistances to NO_2 NH_3 was found at an operating temperature of around 100-250°C.

Author contribution

All authors contributed equally to this work.

Funding

This research received no specific grant from any funding agency in the public, commercial, or not-for-profit sectors.

Data availability statement

The data that support the findings of this study are available on request from the corresponding author.

Conflicts of interest

The authors declare that there is no conflict of interest.

References

[1] H. A. Hadi, R. A. Ismail, N. F. Habubi, Optoelectronic properties of porous silicon heterojunction photodetector, Indian. J. Phys., 88 (2014) 59-63. https://doi.org/10.1007/s12648-013-0375-4

[2] D. H. Jwied, U. M. Nayef, F. A.H. Mutlak, Synthesis of C:Se Nanoparticles Ablated on Porous Silicon for Sensing NO2 and NH3 Gases, Optik, 241 (2021) 167013 .https://doi.org/10.1016/j.ijleo.2021.167013

[3] M. N. Derman, Kh.R. Ahmad, Y. L. Cheong, F. K. Yam, and others, Characteristics of Nanostructure Porous Silicon Prepared by Anodization Technique, Int. J. Electrochem. Sci., 3 (2013) 340 .

[4] J. C. Lin, M. K. Hsu, S. H. Liu, Improvement of Photoluminescence Uniformity of Porous Silicon by using Stirring Anodization process , Eng .Technol. J., 61 (2012)15. https://doi.org/10.5281/zenodo.1075332

[5] J. Xie, S. Lee, X. Chen, Nanoparticle-based theranostic agents, Adv. Drug. Deliv. Rev., 62 (2010) 1064-1079. http://dx.doi.org/10.1016/j.addr.2010.07.009

[6] R. G. Kadhim, R. A. Ismail, W. M. Abdulridha, Structural , Morphological , Chemical and Optical Properties of Porous Silicon Prepared By Electrochemical Etching, Int. J. Thin. Fil. Sci. Tec., 4 (2015) 199–203.

[7] A. Ramizy, Z. Hassan, K. Omar, Porous silicon nanowires fabricated by electrochemical and laser-induced etching, J. Mater. Sci. Mater. Electron., 22 (2011) 717–723.

[8] V. H. Pham, T. Ngugen, A. Ngugen, V. D. Pham, H. Bui, nanoporous silicon microcavity sensor for determination organic solvent and pesticide in water, Adv. Nat. Sci. Nanosci. Nanotechnol., 5 (2014) 045003. https://doi.org/10.1088/2043-6262/5/4/045003

[9] R. Liu, Th. A. Schendake, Y. Y. Li, M. J. Sailor, Y. Fainman, novel porous silicon vapor sensor based on polarization interferometry, Sens. Actuators B Chem., 87 (2002) 58-62. https://doi.org/10.1016/S0925-4005(02)00217-4

[10] H. Saha, porous Silicon sensors-elusive and erudite, Int. J. Smart Sens. Intell. Syst., 1 (2008) 34-56. https://doi.org/10.21307/ijssis-2017-277

[11] M. Kopani , Effect of etching time on structure of p-type porous silicon, Appl. Surf. Sci., 461 (2018) 44–47.

[12] D.H J .wied, U. M. Nayef, F. A.H. Mutlak, Preparation and Characterization of C:Se Nano-Rods Ablated on Porous Silicon, Optik, 239 (2021) 166811. https://doi.org/10.1016/j.ijleo.2021.166811

[13] U.M. Nayef, I. Khudhair, Study of porous silicon humidity sensor vapors by photoluminescence quenching for organic solvents, Optik , 135 (2017) 169–173. https://doi.org/10.1016/j.ijleo.2017.01.060

[14] U. M. Nayef, R. I. Kamel, Enhancement the Electrical Properties of Porous Silicon for Photo-detectors Applications by depositing Bi2O3 nanoparticles, Optik , 207 (2020) 163847. https://doi.org/10.1016/j.ijleo.2019.163847

[15] S. M. Sze, Y. Li, K. K. Ng, Physics of Semiconductor Devices, J. Electr. Electron. Eng. (2006) 944

[16] H. N. Abid, U. M. Nayef, F. A. H. Mutlak, Preparation and characterization Co3O4 nanoparticles on porous Silicon for humidity sensor by photoluminescence, Optik, 178 (2019) 379–383. https://doi.org/10.1016/j.ijleo.2018.09.167